ImmunoHorizons

RESEARCH ARTICLE

Innate Immunity

Bovine Serum Albumin Elicits IL-33–Dependent Adipose Tissue Eosinophilia: Potential Relevance to Ovalbumin-induced Models of Allergic Disease

Heather L. Caslin,[*,†,1] W. Reid Bolus,[*,‡,1] Christopher Thomas,[§] Shinji Toki,[§] Allison E. Norlander,[§,¶] R. Stokes Peebles, Jr.,[§,‖,#] and Alyssa H. Hasty[*,#]

*Department of Molecular Physiology and Biophysics, Vanderbilt University, Nashville, TN; [†]Department of Health and Human Performance, University of Houston, Houston, TX; [‡]Diabetes Center, School of Medicine, University of California San Francisco, San Francisco, CA; [§]Division of Allergy, Pulmonary and Critical Care Medicine, Department of Medicine, Vanderbilt University Medical Center, Nashville, TN; [¶]Department of Anatomy, Cell Biology, and Physiology, Indiana University School of Medicine, Indianapolis, IN; [‖]Department of Pathology, Microbiology, and Immunology, Vanderbilt University School of Medicine, Nashville, TN; and [#]Veterans Affairs, Tennessee Valley Healthcare System, Nashville, TN

ABSTRACT

All cells of the immune system reside in adipose tissue (AT), and increasing type 2 immune cells may be a therapeutic strategy to improve metabolic health. In our previous study using i.p. IL-5 injections to increase eosinophils, we observed that a standard vehicle control of 0.1% BSA also elicited profound AT eosinophilia. In this study, we aimed to determine whether BSA-induced AT eosinophilia results in metabolic benefits in murine models of diet-induced obesity. I.p. 0.1% BSA injections increased AT eosinophils after 4 wk. Despite elevating eosinophils to >50% of immune cells in the AT, body weight and glucose tolerance were not different between groups. Interestingly, BSA elicited epithelial IL-33 production, as well as gene expression for type 2 cytokines and IgE production that were dependent on IL-33. Moreover, multiple models of OVA sensitization also drove AT eosinophilia. Following transplantation of a donor fat pad with BSA-induced eosinophilia, OVA-sensitized recipient mice had higher numbers of bronchoalveolar lavage eosinophils that were recipient derived. Interestingly, lungs of recipient mice contained eosinophils, macrophages, and CD8 T cells from the donor AT. These trafficked similarly from BSA- and non-BSA–treated AT, suggesting even otherwise healthy AT serves as a reservoir of immune cells capable of migrating to the lungs. In conclusion, our studies suggest that i.p. injections of BSA and OVA induce an allergic response in the AT that elicits eosinophil recruitment, which may be an important consideration for those using OVA in animal models of allergic disease. *ImmunoHorizons*, 2023, 7: 842–852.

INTRODUCTION

Immune cells play an important role in adipose tissue (AT) homeostasis (1). Immune cells involved in type 2 inflammation, including Th2 cells, macrophage 2 (M2) cells, group 2 innate lymphoid cells, mast cells, basophils, and eosinophils help to promote healthy expansion and contraction of adipocytes and remodeling of the stromal tissue during lipid storage and

Received for publication August 23, 2023. Accepted for publication November 20, 2023.

Address correspondence and reprint requests to: Dr. Alyssa Hasty, Vanderbilt University, 702 Light Hall, Nashville, TN 37232-0614. E-mail: address: alyssa.hasty@vanderbilt.edu

ORCIDs: 0000-0002-7471-6779 (H.L.C.); 0000-0001-5236-0823 (W.R.B.); 0000-0003-4379-9118 (S.T.); 0000-0002-9357-485X (A.E.N.); 0000-0002-1429-7875 (R.S.P.); 0000-0001-7302-8045 (A.H.H.).

[1]These authors contributed equally to this work.

This work was supported by VA Merit Award I01BX002195 to A.H.H. and by a VI4 Mini Sabbatical Award to W.R.B. A.H.H. is also supported by VA Research Career Scientist Award 5IK6BX005649. While working on this project, W.R.B. was supported by American Heart Association Predoctoral Fellowship 15PRE25560126, and H.L.C. was supported by American Heart Association Postdoctoral Fellowship 20POST35120547. A.E.N. was supported by a National Institutes of Health/National Heart, Lung, and Blood Institute K99/R00 Fellowship (Grant K99HL159594). Adipose tissue transplants were performed in the Vanderbilt Mouse Metabolic Phenotyping Center supported by National Institutes of Health Grant DK059637.

Abbreviations used in this article: alum, aluminum hydroxide; AT, adipose tissue; BAL, bronchoalveolar lavage; HFD, high-fat diet; M2, macrophage 2.

The online version of this article contains supplemental material.

https://doi.org/10.4049/immunohorizons.2300061

ImmunoHorizons is published by The American Association of Immunologists, Inc.

release. However, following weight gain and AT expansion, there is an influx of type 1 immune cells that contribute to the secretion of inflammatory mediators while acting to buffer excess lipid (2). Cytokines such as IL-1β, TNF-α, and IL-6 directly impair insulin signaling and promote adipocyte lipolysis, which eventually lead to ectopic lipid accumulation and the development of type 2 diabetes (3, 4).

Restoring type 2 immunity has been proposed to improve AT homeostasis and dampen metabolic disease following obesity (5, 6). This has been accomplished successfully in mouse models using T regulatory cell manipulations and IL-33 injections (7–10); however, the impact of eosinophil expansion is less straightforward (11). Eosinophilia in IL-5 transgenic mice or with helminth infection was associated with reduced weight gain and glucose intolerance following a high-fat diet (HFD) (12). However, we previously showed that increasing adipose eosinophils via CCR2 deficiency (13) and i.p. recombinant IL-5 injections (14) does not improve glucose tolerance for HFD-fed mice. While conducting the studies above, we observed that BSA, our vehicle control, also elicited substantial AT eosinophilia at a dose of 0.1%. Although we conducted the remaining published studies using a lower dose of BSA, which does not elicit AT eosinophil accumulation, we were interested in further understanding the effects of BSA-induced eosinophilia.

Thus, the primary goal of this study was to understand the mechanism by which BSA induces AT eosinophilia and determine whether this results in reduced body weight and improved glucose tolerance in models of diet-induced obesity. Although BSA did not improve metabolic parameters, we did identify an IL-33–dependent mechanism by which BSA elicits AT eosinophil accumulation. Moreover, we have found that OVA sensitization drives AT eosinophilia and may be an important consideration for those employing the widely used OVA model of allergic disease. Finally, we show that AT eosinophilia increases bronchoalveolar lavage (BAL) eosinophils in a model of OVA challenge and that adipose eosinophils, macrophages, and T cells can traverse from AT to the lungs, suggesting a role for cross-talk between these two organs that may have implications in obesity, allergic lung disease, and more.

MATERIALS AND METHODS

Mouse models

C57BL/6J, BALB/cByJ, and CByJ.SJL(B6)-*Ptprc*^{a}/J mice were purchased from The Jackson Laboratory at 7–10 wk of age and housed in the animal facility at Vanderbilt University for 1 wk to acclimate. Additionally, *Il33*$^{cit/+}$ *and Il33*$^{cit/cit}$ reporter mice (15) were the gift of Dr. Andrew N.J. McKenzie (16). All animal procedures were approved by Vanderbilt's Institutional Animal Care and Use Committee prior to their implementation.

BSA injection model. At 8–12 wk of age, mice were i.p. injected with 250 μl of saline or 0.1% BSA (Sigma-Aldrich, catalog no. A7030) twice weekly for 4 or 8 wk (or as specified in time-course or dose–response experiments). Of note, we have also used BSA (Sigma-Aldrich, catalog no. A8806) with low endotoxin with comparable results to ensure that the effects were not LPS-dependent. Mice were euthanized and tissue was harvested 24 h after the final injection.

Diet induced obesity and glucose tolerance tests. Mice either remained on chow diet or were given ad libitum access to a HFD with 60% kcal from fat (Research Diets, New Brunswick, NJ) for 4–8 wk. A dose response of BSA was completed with i.p. injections twice per week at 0, 0.001, 0.01, and 0.1%. Body composition was measured to obtain lean mass and fat mass by nuclear magnetic resonance using a Bruker Minispec instrument in Vanderbilt's Mouse Metabolic Phenotyping Center during week 4 or 8. Mice were fasted for 6 h during the light cycle for glucose tolerance testing. Fasting blood glucose levels were read using an Accu-Chek Aviva Plus glucometer (Roche) via the tail vein. A 20% glucose solution was administered i.p. at 2 g/kg lean mass, followed by blood glucose readings at 15, 30, 45, 60, 90, and 120 min after glucose injection.

OVA models. Mice were i.p. injected with 250 μl of saline or 0.1% OVA (Sigma-Aldrich, catalog no. A2512) twice a week for 4 wk as in our BSA experiments above. Mice were euthanized and tissue was harvested 24 h after the final injection. To use a more standard OVA model of sensitization (17), mice were i.p. injected at day 0 with OVA–aluminum hydroxide (alum) (100 μl of OVA [10 μg] + alum [20 mg] solution) or alum alone. Mice were euthanized and tissue was harvested on day 14.

Alternaria *model*. Mice were challenged intranasally with 5 μg of *Alternaria* extract (Stallergenes Greer) in 100 μl of PBS or 100 μl of PBS as the vehicle for 4 consecutive days (18). Mice were euthanized and tissue was harvested 24 h after the final challenge.

AT transplants. Donor mice (BALB/cByJ expressing CD45.2) were i.p. injected with 250 μl of saline or 0.1% BSA (Sigma-Aldrich, catalog no. A7030) twice a week for 4 wk to elicit AT with eosinophilia or without. Recipient mice (CByJ.SJL(B6)-*Ptprc*^{a}/J on the BALB/cByJ background expressing CD45.1) were sensitized i.p. with OVA-alum (100 μl of OVA [10 μg] + alum [20 mg] solution). One week following sensitization, donor mice were euthanized and one epididymal adipose fat pad was transplanted into the peritoneal cavity of each recipient mouse with the help of Vanderbilt's Mouse Metabolic Phenotyping Center. One week following transplantation (14 d following sensitization), recipient mice were challenged with 1% OVA-PBS solution created by an ultrasonic nebulizer for 40 min each day for 3 d. Mice were euthanized and tissue was harvested 24 h after the final challenge.

Immune cell isolation

Adipose stromal vascular fraction isolation. Adipose tissue was excised, weighed on a Mettler Toledo scale, and minced in a

https://doi.org/10.4049/immunohorizons.2300061

1% FBS/PBS solution. AT was then digested with 2 mg/ml type II collagenase (Sigma-Aldrich, catalog no. C6885) for 40 min at 37°C. Digested AT was then diluted in 1% FBS/PBS, vortexed, and passed through a 100-μm filter. Following centrifugation, RBCs were lysed with ACK (ammonium-chloride-potassium) lysis buffer and remaining stromal vascular cells were passed through 35-μm filters for further analysis.

Lung immune cell isolation. Lung tissue was excised, weighed on a Mettler Toledo scale, and minced in a 5% FBS/RPMI 1640 solution. Lung tissue was then digested with 0.5 mg/ml type IV collagenase (Worthington Biochemical, catalog no. LS004188) plus DNase (2 μg/ml) for 25 min at 37°C. EDTA (1:100) was added to stop digestion and cells were vortexed and forced through a 100-μm filter with a syringe. After centrifugation, RBCs were lysed with ACK lysis buffer and the remaining cells were passed through 35-μm filters for further analysis.

Blood cell isolation. Approximately 200 μl of blood was collected retro-orbitally in heparinized capillary tubes. Blood was diluted with 2 ml of deionized water in a 15-ml conical tube and mixed by inverting for 15 s to lyse RBCs. The reaction was neutralized by dilution with 10 ml of 1% FBS/PBS, centrifuged, and decanted; the cell pellet was resuspended and used for further analysis.

BAL fluid isolation. The trachea was isolated and cleaned and then a small incision was made for an endotracheal tube insertion. Saline (800 μl) was instilled into the lungs and then aspirated from the airways using the same syringe. Samples were excluded for four mice with bloody BAL, which required ACK lysis.

Flow cytometry

Isolated immune cells were first incubated with purified rat anti-mouse CD16/CD32 Fc Block (1:200, BD Biosciences, catalog no. 553141) for 5–10 min on ice. Cells were stained at 1:200 or as noted for 30 min at 4°C, while protected from light, with a combination of fluorophore-conjugated Abs as follows: BV510 anti-mouse CD45 (BioLegend, catalog no. 103137), allophycocyanin-Cy7 anti-mouse CD45 (BioLegend, catalog no. 103116), allophycocyanin anti-mouse CD45.1 (BioLegend, catalog no. 110714), BV510 anti-mouse CD45.2 (BioLegend, catalog no. 109839), BV711 anti-mouse CD11b (BD Biosciences, catalog no. 563168), FITC anti-mouse CD11b (BD Biosciences, catalog no. 553310), PE anti-mouse Siglec-F (BD Biosciences, catalog no. 552126), BV421 anti-mouse Siglec-F (BD Biosciences, catalog no. 562681), PerCP-Cy5.5 anti-mouse Ly6C (BD Biosciences, catalog no. 560525), allophycocyanin-Cy7 anti-mouse F480 (BioLegend, catalog no. 123118), PE anti-mouse Ly6G (BioLegend, catalog no. 127607), allophycocyanin-Cy7 anti-mouse TCRb (BD Biosciences, catalog no. 562681), AF700 anti-mouse CD4 (BD Biosciences, catalog no. 116022), FITC anti-mouse CD8 (BD Biosciences, catalog no. 553031), AF647 anti-mouse CD19 (BD Biosciences, catalog no. 557684), FITC anti-mouse B220 (BD Biosciences, catalog no. 553088), allophycocyanin-Cy7 anti-mouse CD117 (BioLegend, catalog no. 105825), allophycocyanin anti-mouse FcεR1 (BioLegend, catalog no. 134315), BV711 anti-mouse CD103 (BioLegend, catalog no. 121435), BV605 anti-mouse EpCAM (BioLegend, catalog no. 118227), and PE-Cy7 anti-mouse CD31 (BioLegend, catalog no. 102418). Cells were washed several times, counting beads were added (Count-Bright absolute counting beads, Thermo Fisher Scientific, catalog no. C36950), and cells were stained with viability dye (1 μg/ml DAPI or propidium iodide) just before flow cytometric analysis. Cells were analyzed on a four-laser BD LSRFortessa (BD Biosciences) in the Vanderbilt Flow Cytometry Shared Resource or on the Miltenyi Biotec MACSQuant 10 in our laboratory. Results were analyzed using FlowJo software with the following gating scheme: forward scatter/side scatter (debris removed), forward scatter height/forward scatter area (single cells), propidium iodide or DAPI (live), and $CD45^{+/-}$/1.1/1.2 as required by the experiment. The following markers were then used for each cell population: AT eosinophils ($CD11b^{+}$Siglec-F^{+}), lung eosinophils ($CD11b^{+}$Siglec-F^{mod}), lung alveolar macrophages ($CD11b^{lo}$Siglec-F^{hi}), myeloid cells ($CD11b^{+}$), classical monocytes ($CD11b^{+}Ly6C^{hi}$), macrophages ($CD11b^{+}F480^{+}$), neutrophils ($Ly6G^{+}$), T cells ($TCRb^{+}$), CD4 T cells ($TCRb^{+}CD4^{+}$), CD8 T cells ($TCRb^{+}CD8^{+}$), B cells ($CD19^{+}B220^{+}$), mast cells ($CD117^{+}FcεR1^{+}$), dendritic cells ($CD103^{+}$), epithelial cells ($CD45^{-}EpCAM^{+}$), and endothelial cells ($CD45^{-}CD31^{+}$).

BAL inflammatory cell analysis

Total cells were counted from each BAL collection using a hemocytometer. BAL fluid (100 μl) was then cytospun. Slides were stained with a three-step stain kit (Epredia). Cell differential counts were performed by an investigator blinded to the experimental groups using staining and morphology to classify the cells as macrophages, eosinophils, leukocytes, and neutrophils.

Quantitative PCR

Tissues were homogenized in TRIzol, and RNeasy mini kits (Qiagen, catalog no. 74104) were used to isolate RNA according to the manufacturer's instructions. Purified RNA was reverse transcribed into cDNA by iScript RT (Bio-Rad, catalog no. 1708841), and gene expression was quantified using a FAM-conjugated TaqMan gene expression assay (Life Technologies) and iQ Supermix (Bio-Rad, catalog no. 1708862). Data were normalized to 18S using the $2^{-\Delta\Delta Ct}$ method.

Statistical analysis

All statistical graphs and analyses were performed in GraphPad Prism 9.0 software. Statistical tests include a Student *t* test, a one-way ANOVA with a post hoc test for multiple comparisons, and a two-way ANOVA with a post hoc test for multiple comparisons. Prior to statistical analysis, any outliers were removed by the ROUT method, with $Q = 5\%$. Significance was defined by a p value of 0.05.

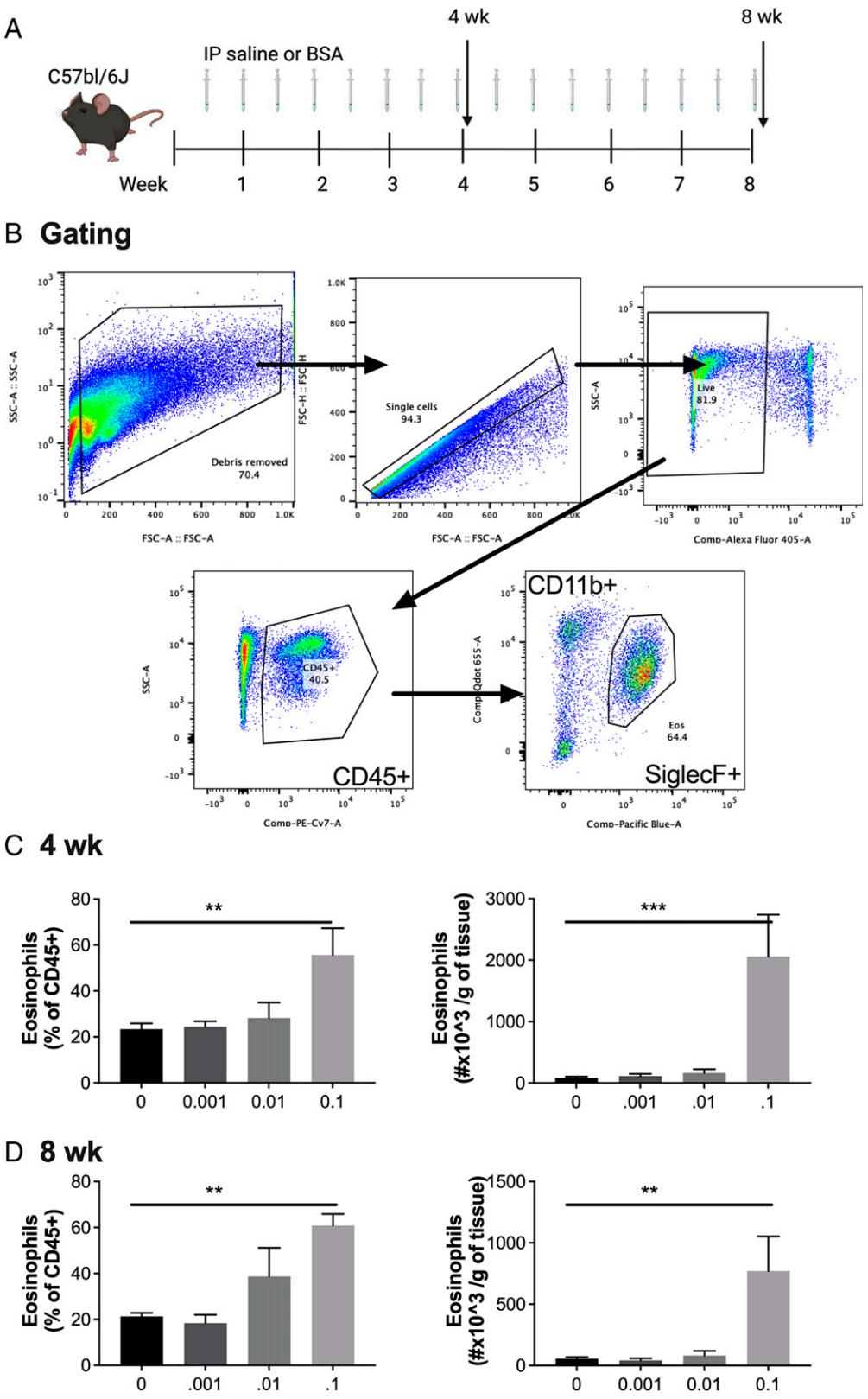

FIGURE 1. I.p. BSA injections induce AT eosinophilia in C57BL/6J mice.
(**A**) Schematic of study design. BSA was injected i.p. twice weekly at 0–0.1% for 4 or 8 wk in C57BL/6J male mice. (**B**) Representative gating strategy/flow plots for adipose tissue eosinophils. (**C** and **D**) Percent and number of eosinophils per gram of fat were quantified at (C) 4 and (D) 8 wk by flow cytometry. Data represent the mean ± SEM of 4–10 mice/group and each experiment was completed twice. $^{**}p < 0.01$, $^{***}p < 0.001$ by one-way ANOVA and a Dunnett multiple comparison test.

https://doi.org/10.4049/immunohorizons.2300061

RESULTS

Repeated exposure to low-dose BSA induces adipose eosinophilia in C57BL/6J mice

To experimentally test our previous observation that low-dose BSA, often used as a carrier protein, can induce AT eosinophilia, C57BL/6J mice were i.p. injected with 250 μl of saline or BSA (0.001, 0.01, and 0.1%) twice weekly for 4 or 8 wk (Fig. 1A). Flow cytometry was used to quantify eosinophils, and a representative flow plot can be found in Fig. 1B. After both 4 and 8 wk of treatment, a concentration of at least 0.1% BSA treatment was required to significantly increase the percent and total number of AT eosinophils (Fig. 1C, 1D). Strikingly, this increase in eosinophils accounted for more than half of the entire epididymal AT immune cell milieu ($CD45^+$ leukocytes), a 3-fold increase from ∼20% at baseline to ∼60% with BSA treatment.

BSA-induced AT eosinophilia does not protect against diet-induced obesity or glucose intolerance

Whether AT eosinophilia can improve systemic glucose intolerance associated with obesity is dependent on the model used (11). Thus, we sought to determine whether BSA-induced AT eosinophilia could protect against weight gain and glucose intolerance following HFD feeding. C57BL/6J mice were fed a 60% HFD for either 4 or 8 wk and 250 μl of saline or 0.1% BSA was injected twice per week for the duration of the diet (Fig. 2A). By 4 wk, there was a trend toward increased AT eosinophilia (Fig. 2B) with no difference in body weight gain (Fig. 2C) or glucose tolerance (Fig. 2D). After 8 wk, 0.1% BSA significantly increased adipose eosinophils as a percent of total leukocytes and as number per gram of tissue (Fig. 2E). Even with this large influx of eosinophils, there was no difference in body weight gain (Fig. 2F) or glucose tolerance (Fig. 2G) compared with saline-injected controls.

BSA increases AT, lung, and blood eosinophils in BALB/c mice

Although a dramatic increase in AT eosinophils was not protective against metabolic disease, eosinophils are often involved in the pathogenesis of Th2-mediated diseases such as allergy and asthma (19). Thus, we also confirmed our results in BALB/c mice (Fig. 3A, schematic), which are Th2 prone and more susceptible to the development of asthma and allergy (20). As in

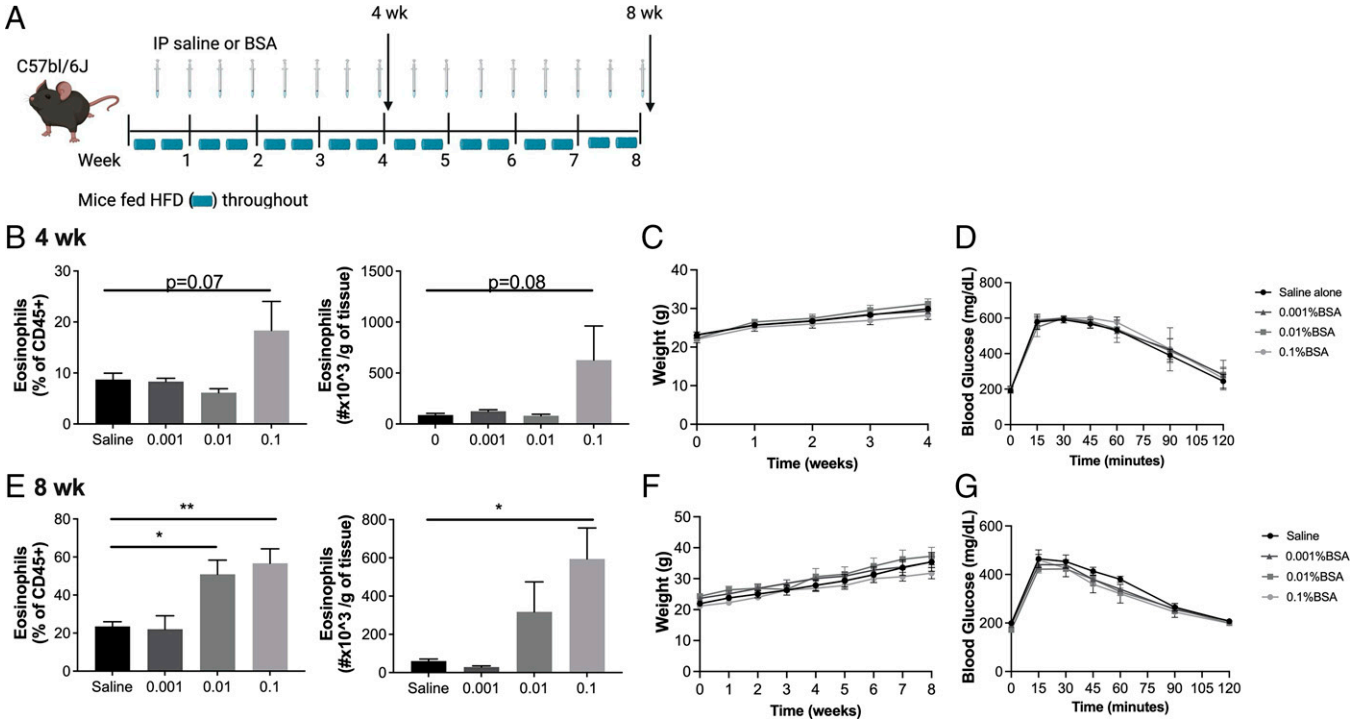

FIGURE 2. BSA-induced AT eosinophil accumulation does not protect against diet-induced obesity or glucose intolerance in C57BL/6J mice. (**A**) Schematic of study design. Male C57BL/6J mice were placed on a high-fat diet (HFD) for 4 or 8 wk and BSA was injected i.p. twice weekly at a concentration of 0–0.1% during the course of the study. (**B** and **E**) Adipose tissue eosinophils were quantified by flow cytometry at the end of the 4 (B) or 8 wk (E) study and are presented as percent of $CD45^+$ cell and as number per gram of tissue. (**C** and **F**) Body weight of mice during the 4- and 8-wk studies. (**D** and **G**) Glucose tolerance tests were performed at 4 and 8 wk using 2 g/kg body weight of dextrose injected i.p. Data represent the mean ± SEM of 4–10 mice/group, and each experiment was completed twice. *$p < 0.05$, **$p < 0.01$ by one-way ANOVA and a Dunnett multiple comparison test (B and E) or two-way ANOVA (C, D, F, and G).

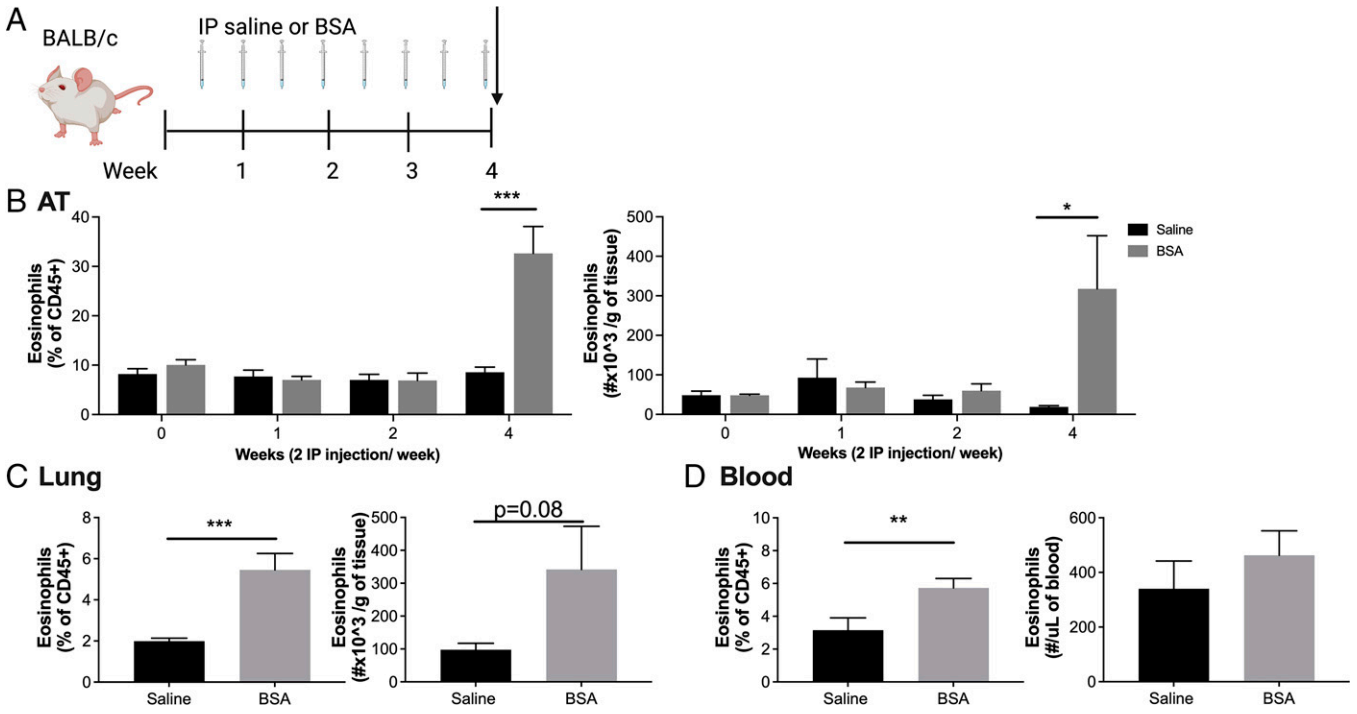

FIGURE 3. BSA injections induce eosinophil accumulation in the adipose tissue and lungs of BALB/c mice.

(**A**) Schematic of study design. BSA was injected i.p. twice weekly at 0.1% for up to 4 wk in BALB/c male mice. (**B**–**D**) The percent and number of eosinophils were quantified by flow cytometry in (B) epididymal adipose tissue, (C) lung, and (D) blood at the end of the 4-wk study. Data represent the mean ± SEM of 9–12 mice/group and each experiment was completed twice. *$p < 0.05$, **$p < 0.01$, ***$p < 0.001$ by a two-way ANOVA and a Bonferroni post hoc test (B) or *t* test (C and D).

C57BL/6J mice, there was a significant increase of eosinophils in AT by percent and number per gram after 4 wk of BSA exposure (Fig. 3B). Additionally, there was a significant increase in the percent of eosinophils in the lung (Fig. 3C) and blood (Fig. 3D). Eosinophils increased as percent and number per gram of total AT immune cells ($CD45^+$), and there was

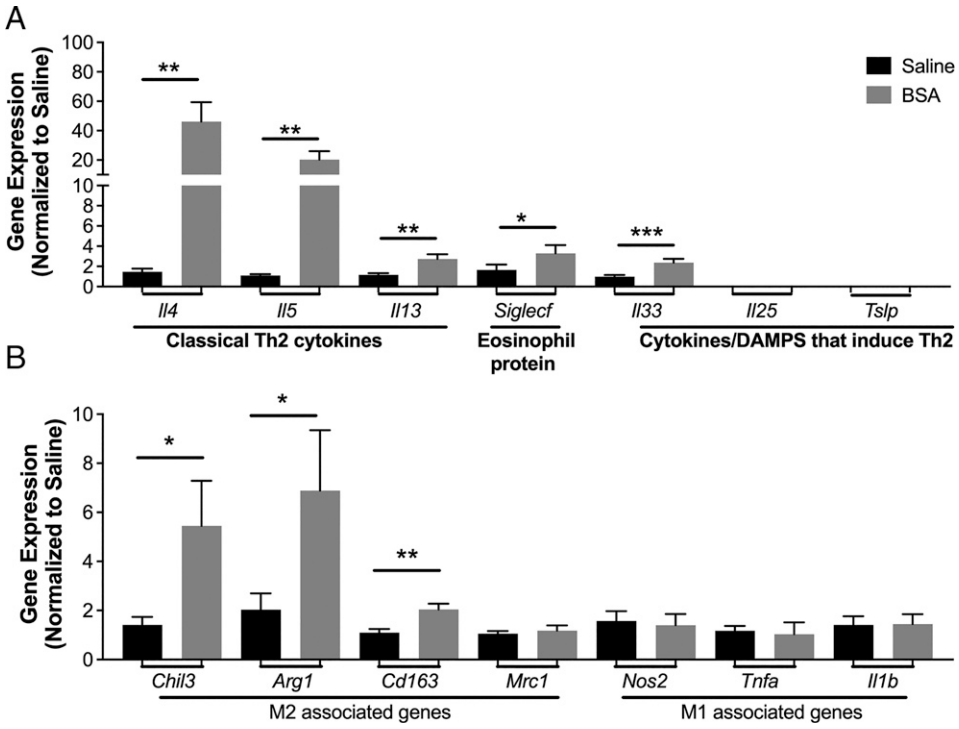

FIGURE 4. BSA induces type 2 gene expression in the adipose tissue.

BSA was injected i.p. twice weekly at 0.1% for 4 wk in BALB/c males. (**A**) Th2-associated genes and (**B**) macrophage 1 (M1)–like and M2-like genes were assessed by quantitative PCR. Data represent the mean ± SEM of $n = 10–12$/group from two experiments. *$p < 0.05$, **$p < 0.01$, ***$p < 0.001$ by *t* test.

https://doi.org/10.4049/immunohorizons.2300061

a compensatory reduction in AT macrophages by percent (Supplemental Fig. 1); however, no other immune cell population analyzed in the AT (Supplemental Fig. 1) and lung (Supplemental Fig. 2) showed a significant change.

BSA induces a type 2 allergic response, partly dependent on IL-33

To further explore whether AT eosinophilia is driven by Th2-mediated processes, we analyzed gene expression across a panel of type 2 genes in mice treated with saline or BSA during 4 wk. There was a significant increase in multiple Th2 cytokines (*Il4*, *Il5*, and *Il13*) as well as *Siglecf* (eosinophil-specific marker) and *Il33* (eosinophil activation/recruitment) with BSA treatment (Fig. 4A). Moreover, there was a significant increase in M2-associated genes (*Chil3*, *Arg1*, and *Cd163*; Fig. 4B).

IL-33 can be released from damaged epithelial cells as an alarmin, initiating Th2 polarization and activating group 2 innate lymphoid cells, eosinophils, and mast cells in allergic development. Using *Il33*$^{cit/+}$ fluorescent reporter mice that express the citrine gene directly downstream of the ATG start codon of *Il33* (15), we found that citrine expression was elevated in the AT stromal epithelial cells (CD45$^-$EpCAM$^+$) following BSA injections (Fig. 5A). There were no differences in citrine expression in other adipose populations (shown in Fig. 5A) or adipose FcεR1$^+$ cells (data not shown). Additionally, there were no differences in any lung populations (data not shown). As the *Il33*$^{cit/cit}$ mice can also be used as IL-33–deficient mice (15), we found that without functional IL-33, BSA did not induce significant eosinophilia in the AT (Fig. 5B) or blood (Fig. 5C). Moreover, whereas IgE levels in the blood were significantly

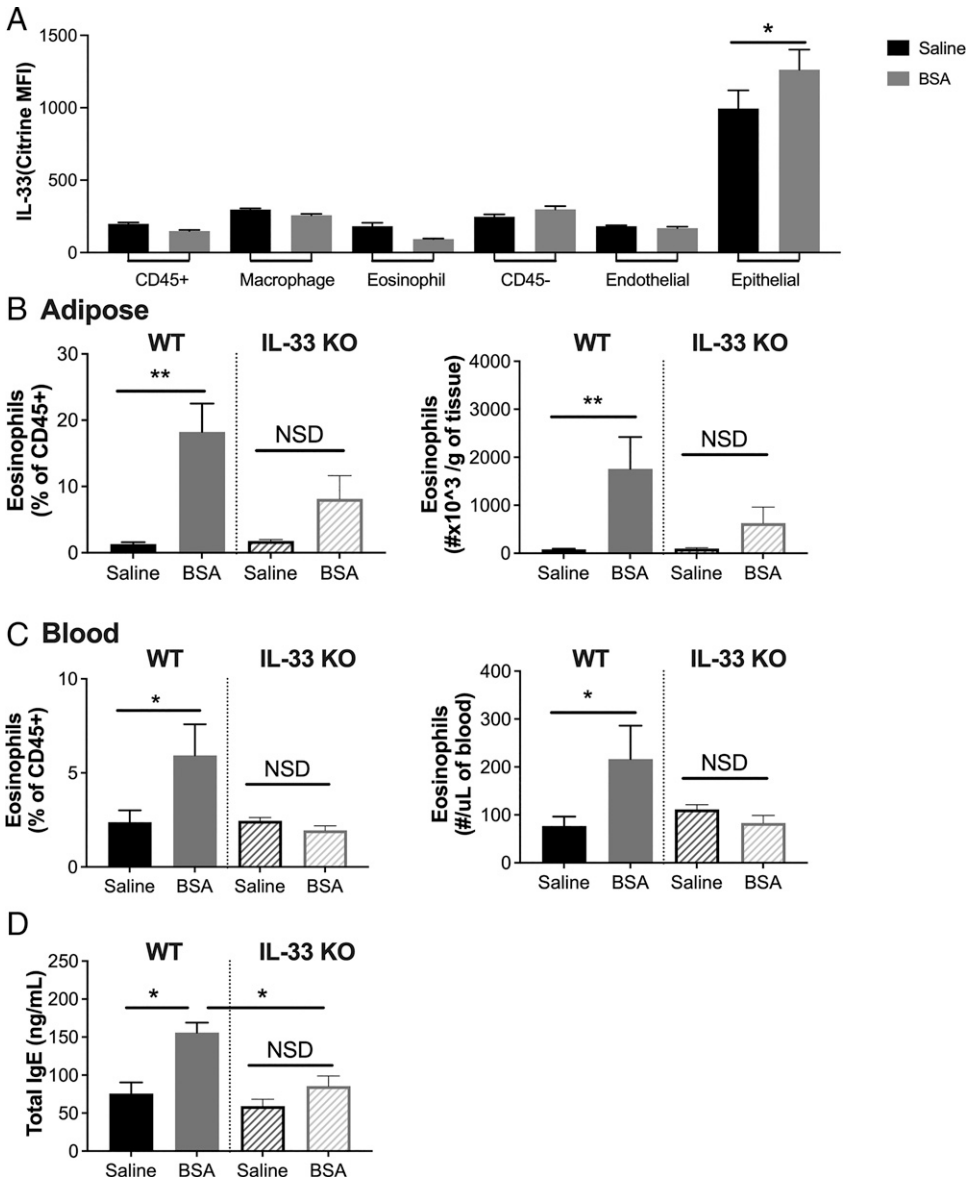

FIGURE 5. The induction of eosinophil accumulation by BSA is partially driven by epithelial IL-33.

(**A**) BSA was injected i.p. twice weekly at 0.1% for 4 wk in male and female IL-33 reporter (het) mice. Citrine expression was assessed in the adipose tissue by flow cytometry, and the indicated IL-33 is primarily expressed in epithelial cells. BSA was injected twice weekly at 0.1% for 4 wk in WT BALB/c or IL-33 knockout (KO) male and female mice. (**B** and **C**) Percent and number of eosinophils were quantified by flow cytometry in (B) adipose tissue and (C) blood. (**D**) IgE was measured in the blood. Data represent the mean ± SEM of n = 5–12/group from two experiments. *$p < 0.05$, **$p < 0.01$ by a t test (A) or one-way ANOVA and Tukey pairwise comparisons (B–D). NSD, no statistical difference.

elevated with BSA treatment in WT mice, this was significantly reduced in IL-33–deficient mice (Fig. 5D).

OVA of standard allergy models also induces AT eosinophilia

OVA is a protein that has historically been used as an Ag in mouse models of allergic disease; thus, the potential for OVA to induce AT accumulation of eosinophils is relevant to this disease model (20). Following the same injection protocol as for BSA (Fig. 6A), we found that i.p. OVA injections also elicit eosinophilia in AT (Fig. 6B) and lung (Fig. 6C). This model is a fairly high dose of albumin, and many standard protocols elicit allergic disease using a lower dose alongside the adjuvant (17, 20). Thus, BALB/c mice were i.p. injected with alum (20 mg) or OVA (10 μg) + alum (20 mg) (Fig. 6D). After 14 d, mice receiving OVA + alum demonstrated increased AT eosinophils compared with alum alone (Fig. 6E).

As many scientists are moving away from OVA models due to limitations in translation to human allergy (21), we also explored an *Alternaria* extract model of allergy with 4 d of intranasal sensitization and challenge following saline or BSA injections as above (Supplemental Fig. 3A and Ref. 18). While BSA increased eosinophils in the AT compared with saline treatment as expected, *Alternaria* exposure itself did not increase AT eosinophilia and BSA-induced eosinophilia was not augmented by *Alternaria* exposure (Supplemental Fig. 3B). To examine the effect of BSA-induced eosinophilia on the response of other immune populations to *Alternaria* in the lung, we compared saline- and BSA-treated groups challenged with *Alternaria*. The only significant difference in lung populations was a reduction in macrophages ($CD11b^+F480^+$) in the BSA-treated group (Supplemental Fig. 3C). However, the increase in lung eosinophils, alveolar macrophages, total macrophages, and neutrophils was also blunted following BSA treatment (Supplemental Fig. 3D–F).

Adipose eosinophilia increases BAL eosinophilia in a transplant model

To determine whether an increase in AT eosinophils impacts allergic responses of the lung, CD45.2 donors were given BSA to induce AT eosinophilia and then this epididymal AT was transplanted into CD45.1 recipient mice sensitized with OVA-alum. Fourteen days following sensitization and 1 wk following transplantation, recipients were challenged with OVA inhalation over 3 d (Fig. 7A). Whereas the total AT immune cells and eosinophils were not different in the recipient AT 1 wk after transplant and OVA challenge, more donor eosinophils persisted in the transplanted AT from the BSA-injected donor mice than the saline-injected controls (Supplemental Fig. 4A–C). In contrast, donor adipose of saline-injected controls, once transplanted, was more heavily repopulated by eosinophils of recipient mice than donor adipose of BSA-injected mice (Supplemental Fig. 4C). Lung BAL fluid of recipients transplanted with hypereosinophilic AT from BSA donors had increased BAL eosinophils

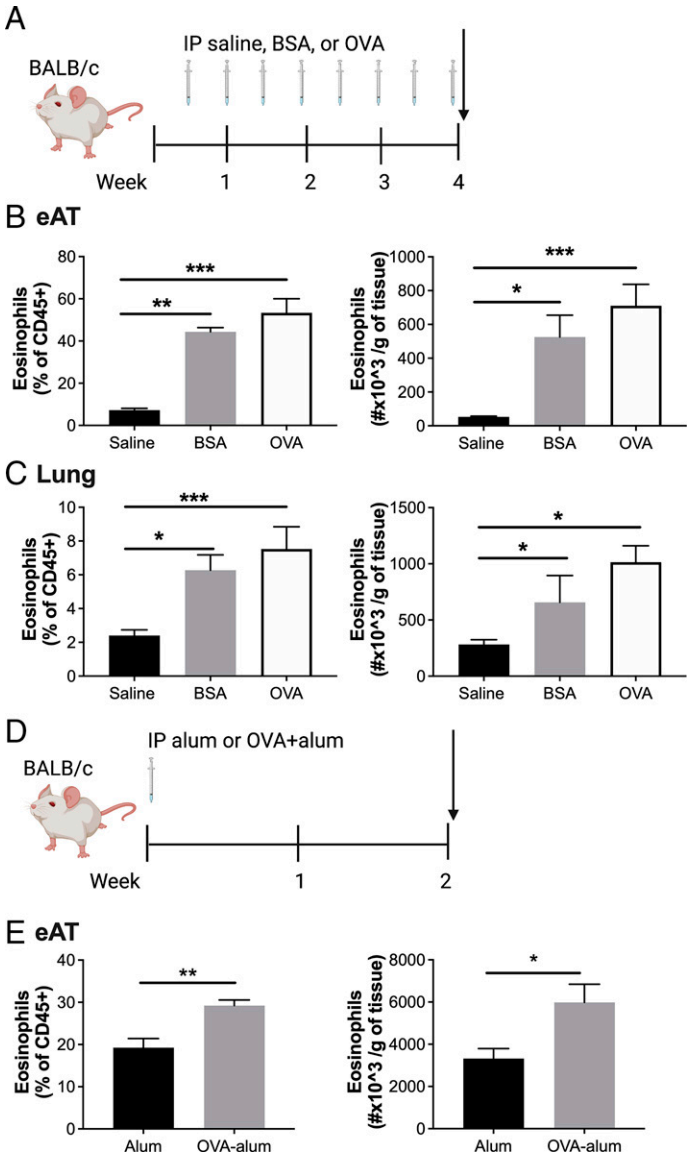

FIGURE 6. Intraperitoneal injection of OVA induces adipose tissue eosinophil accumulation.

(**A**) Schematic of study design. BSA or OVA were injected i.p. twice weekly at 0.1% for 4 wk in BALB/c male mice. (**B** and **C**) Percent and number of eosinophils were quantified by flow cytometry in (B) epididymal adipose tissue and (C) lung. (**D**) Schematic of study design. OVA (10 μg) + alum (20 mg) or alum (20 mg) was injected once in BALB/c male and female mice. (**E**) At day 14, percent and number of eosinophils were quantified by flow cytometry in epididymal adipose tissue. Data represent the mean ± SEM of $n = 4$/group in saline and BSA groups and $n = 8$–13/group in the OVA groups. Experiments were repeated twice. $^*p < 0.05$, $^{**}p < 0.01$, $^{***}p < 0.001$ by one-way ANOVA with a Dunnett multiple comparison test (B and C) or *t* test (E).

(Fig. 7B) compared with BAL of mice with control AT transplants. This was confirmed by flow cytometry (Fig. 7C, 7D). Interestingly, all BAL eosinophils were CD45.1 recipient cells (Fig. 7E), indicating that the elevated BAL eosinophils were

https://doi.org/10.4049/immunohorizons.2300061

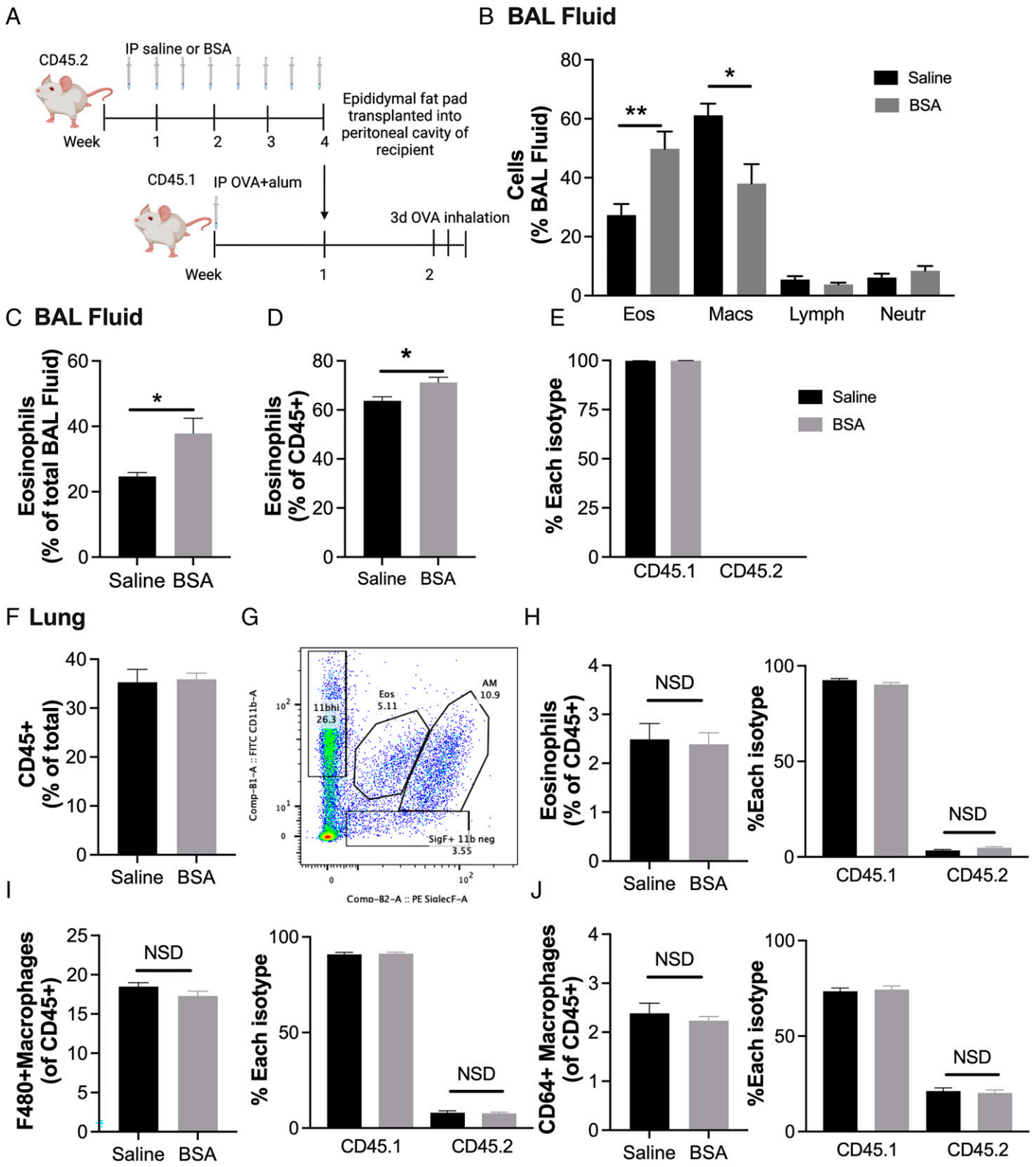

FIGURE 7. Adipose transplants from BSA treated mice increase recipient BAL eosinophils following OVA challenge in recipient mice.

(**A**) Schematic of study design. Saline or 0.1% BSA was injected into male BALB/c (CD45.2) donors for 4 wk. Epididymal adipose tissue from these donor mice was then transplanted into the peritoneal cavity of male CD45.1 recipients who had received OVA (10 μg) + alum (20 mg) 1 wk prior. After one additional week of OVA + alum injection, all mice inhaled OVA for 45 min for 3 d. (**B**) BAL differential counts by Giemsa staining. (**C**) Percent eosinophils of all BAL cells. (**D**) Percent eosinophils of $CD45^+$ BAL cells. (**E**) Percent of each eosinophil isotype (CD45.1 or CD45.2) in BAL. ***(Continued)***

https://doi.org/10.4049/immunohorizons.2300061

not directly derived from the transplanted AT, but rather a secondary effect. Moreover, although there was no difference in total $CD45^+$ cells in the lung tissue itself (Fig. 7F), the lung eosinophils (Fig. 7G, 7H), or any other lung populations following transplant and challenge (Fig. 7I, 7J, Supplemental Fig. 4D–I), there were donor eosinophils (Fig. 7H), $F480^+$ and $F480^+$ $CD64^+$ macrophage populations (Fig. 7I, 7J), and $CD8^+$ T cells (Supplemental Fig. 4I), suggesting trafficking from all donor AT to the lung.

DISCUSSION

We previously observed that BSA, as a vehicle control for rIL-5, elicited AT eosinophilia at a dose of 0.1%. Here, we found that IP injections of 0.1% BSA twice per week for 4 wk elicits eosinophil accumulation in the gonadal AT. Despite consistently making up more than >40% of the AT immune cells, adipose eosinophilia provided no benefits to systemic metabolism. This supported our previous findings where IL-5–driven eosinophilia was also not protective against weight gain or glucose intolerance (14), despite improvements following helminth or transgenic-driven increases in AT eosinophils shown by others (12, 22). We have published a commentary outlining a few differences between our studies and others (11), which includes whether eosinophils are systemically elevated through the lifetime of the mouse versus recruited just to the adipose tissue prior to or following HFD feeding. We hope to see further research continue to evaluate how the source (tissue-resident progenitor cells versus bone marrow), polarization status, activation signals, and distribution of eosinophils may influence metabolic protection. Importantly, others are also beginning to recognize the heterogeneity of eosinophils in other disease contexts, and further understanding of this heterogeneity will be important for therapeutic development across many medical fields (23).

We found that adipose eosinophil accumulation occurs via the induction of type 2 immune pathways (24, 25). BSA elicits IL-33 production by AT epithelial cells as well as gene expression for type 2 cytokines (*Il4*, *Il5*, *Il13*), M2 macrophage polarization genes (*Chil3*, *Arg1*, *Cd163*), and IgE production, suggesting that BSA induces an allergic response. However, it is noteworthy that we did not measure BSA-specific IgE. Adipose eosinophilia and IgE production were reduced in IL-33–deficient mice, suggesting that adipose eosinophilia is partially dependent on IL-33 release. Interestingly, allergy to bovine meat, and specifically BSA, can be considered a cause of eosinophilic esophagitis in humans, as presented in a case study (26). Moreover, it has been previously shown that AT macrophages can function as APCs by i.p. injection of FITC-labeled OVA (27). One hour following the injection, the OVA was detectable in adipose macrophages throughout visceral fat and in fat-associated lymphoid clusters. Four weeks following the initial injection, we did not detect a change in adipose macrophage, T cell, or B cell number; however, it is plausible that similar Ag presentation may occur in our model to mediate the early cytokine response with the induction of adaptive immunity and IgE production.

Our findings suggest that multiple sources of albumin can induce AT eosinophilia as shown by both BSA or OVA injections and in a more standard model of OVA-alum sensitization (17). Importantly, we did not see that *Alternaria* extract inhalation induced AT eosinophilia, suggesting a specificity to BSA i.p. injections. However, we did find that BSA injections dampen *Alternaria* extract–induced cell migration to the lung, and we found that following transplantation of a donor adipose fat pad with BSA-induced eosinophilia, BAL eosinophil numbers are higher following OVA challenge. Moreover, we showed that some donor adipose immune cells trafficked into the lung (eosinophils, macrophages, and $CD8^+$ T cells); however, there was no difference in trafficking based on donor adipose tissue eosinophilia. This study did not further characterize the recruited cells (e.g., the state of macrophage polarization); however, future studies exploring the polarization and activation of the recruited cells may reveal previously unappreciated biology. Importantly, this work contributes (to our knowledge) new evidence that innate immune cells can traffic out of the adipose, which has recently been shown with adipose macrophage trafficking to the eye and brain (28, 29). Taken together, these studies support a broader role for AT immune cells in metabolic and inflammatory diseases.

In conclusion, i.p. BSA and OVA injections induce sensitization and AT eosinophilia that is IL-33–dependent. This may be of interest to those who use OVA models of allergic disease. Sensitization is often attributed to draining lymph nodes, especially in inhalation models, but our data support the notion that most i.p. injection models likely induce systemic sensitization (21). Moreover, these data suggest additional rationale for why many allergy researchers have begun to move away from OVA and toward models such as the house dust mite, adding to a list of what others have noted: OVA is not a human Ag, it does not replicate chronic allergic asthma, and it does not require IgE and mast cells when OVA is administered with alum (19, 21). Lastly, our work adds to the growing list of studies suggesting that immune cells can traffic not only in, but also out of the fat, suggesting a role for the AT as an immune cell reservoir.

(**F**) Lung $CD45^+$ cells were quantified by flow cytometry. (**G**) Gating for lung eosinophils and alveolar macrophages by CD11b and Siglec-F. (**H**–**J**) Percent of $CD45^+$ and percent of CD45.1 and CD45.2 were quantified for (H) eosinophils, (I) $F480^+$ macrophages, and (J) $CD64^+F480^+$ macrophages. Data represent the mean ± SEM of 7–8/group for BAL samples and 9–10/group for lung samples. *$p < 0.05$, **$p < 0.01$ by *t* test. NSD, no statistical difference.

https://doi.org/10.4049/immunohorizons.2300061

DISCLOSURES

The authors have no financial conflicts of interest.

REFERENCES

1. Trim, W. V., and L. Lynch. 2022. Immune and non-immune functions of adipose tissue leukocytes. *Nat. Rev. Immunol.* 22: 371–386.
2. Wensveen, F. M., S. Valentić, M. Šestan, T. Turk Wensveen, and B. Polić. 2015. The "Big Bang" in obese fat: events initiating obesity-induced adipose tissue inflammation. *Eur. J. Immunol.* 45: 2446–2456.
3. Gao, D., M. Madi, C. Ding, M. Fok, T. Steele, C. Ford, L. Hunter, and C. Bing. 2014. Interleukin-1β mediates macrophage-induced impairment of insulin signaling in human primary adipocytes. *Am. J. Physiol. Endocrinol. Metab.* 307: E289–E304.
4. Hotamisligil, G. S., D. L. Murray, L. N. Choy, and B. M. Spiegelman. 1994. Tumor necrosis factor alpha inhibits signaling from the insulin receptor. *Proc. Natl. Acad. Sci. USA* 91: 4854–4858.
5. Schmidt, V., A. E. Hogan, P. G. Fallon, and C. Schwartz. 2022. Obesity-mediated immune modulation: one step forward, (Th)2 steps back. *Front. Immunol.* 13: 932893.
6. Bolus, W. R., and A. H. Hasty. 2019. Contributions of innate type 2 inflammation to adipose function. *J. Lipid Res.* 60: 1698–1709.
7. Cipolletta, D., M. Feuerer, A. Li, N. Kamei, J. Lee, S. E. Shoelson, C. Benoist, and D. Mathis. 2012. PPAR-γ is a major driver of the accumulation and phenotype of adipose tissue Treg cells. *Nature* 486: 549–553.
8. Eller, K., A. Kirsch, A. M. Wolf, S. Sopper, A. Tagwerker, U. Stanzl, D. Wolf, W. Patsch, A. R. Rosenkranz, and P. Eller. 2011. Potential role of regulatory T cells in reversing obesity-linked insulin resistance and diabetic nephropathy. *Diabetes* 60: 2954–2962.
9. Saxton, S. N., A. S. Whitley, R. J. Potter, S. B. Withers, R. Grencis, and A. M. Heagerty. 2020. Interleukin-33 rescues perivascular adipose tissue anticontractile function in obesity. *Am. J. Physiol. Heart Circ. Physiol.* 319: H1387–H1397.
10. Miller, A. M., D. L. Asquith, A. J. Hueber, L. A. Anderson, W. M. Holmes, A. N. McKenzie, D. Xu, N. Sattar, I. B. McInnes, and F. Y. Liew. 2010. Interleukin-33 induces protective effects in adipose tissue inflammation during obesity in mice. *Circ. Res.* 107: 650–658.
11. Bolus, W. R. 2018. Diversity of adipose tissue immune cells: are all eosinophils created equal? *BioEssays* 40: e1800150.
12. Wu, D., A. B. Molofsky, H.-E. Liang, R. R. Ricardo-Gonzalez, H. A. Jouihan, J. K. Bando, A. Chawla, and R. M. Locksley. 2011. Eosinophils sustain adipose alternatively activated macrophages associated with glucose homeostasis. *Science* 332: 243–247.
13. Bolus, W. R., D. A. Gutierrez, A. J. Kennedy, E. K. Anderson-Baucum, and A. H. Hasty. 2015. CCR2 deficiency leads to increased eosinophils, alternative macrophage activation, and type 2 cytokine expression in adipose tissue. *J. Leukoc. Biol.* 98: 467–477.
14. Bolus, W. R., K. R. Peterson, M. J. Hubler, A. J. Kennedy, M. L. Gruen, and A. H. Hasty. 2018. Elevating adipose eosinophils in obese mice to physiologically normal levels does not rescue metabolic impairments. *Mol. Metab.* 8: 86–95.
15. Hardman, C. S., V. Panova, and A. N. J. McKenzie. 2013. IL-33 citrine reporter mice reveal the temporal and spatial expression of IL-33 during allergic lung inflammation. *Eur. J. Immunol.* 43: 488–498.
16. Stier, M. T., R. Mitra, L. E. Nyhoff, K. Goleniewska, J. Zhang, M. V. Puccetti, H. C. Casanova, A. C. Seegmiller, D. C. Newcomb, P. L. Kendall, et al. 2019. IL-33 is a cell-intrinsic regulator of fitness during early B cell development. *J. Immunol.* 203: 1457–1467.
17. Zhou, W., J. Zhang, K. Goleniewska, D. E. Dulek, S. Toki, D. C. Newcomb, J. Y. Cephus, R. D. Collins, P. Wu, M. R. Boothby, and R. S. Peebles, Jr. 2016. Prostaglandin I_2 suppresses proinflammatory chemokine expression, CD4 T cell activation, and STAT6-independent allergic lung inflammation. *J. Immunol.* 197: 1577–1586.
18. Toki, S., K. Goleniewska, J. Zhang, W. Zhou, D. C. Newcomb, B. Zhou, H. Kita, K. L. Boyd, and R. S. Peebles, Jr. 2020. TSLP and IL-33 reciprocally promote each other's lung protein expression and ILC2 receptor expression to enhance innate type-2 airway inflammation. *Allergy* 75: 1606–1617.
19. Jacobsen, E. A., N. A. Lee, and J. J. Lee. 2014. Re-defining the unique roles for eosinophils in allergic respiratory inflammation. *Clin. Exp. Allergy* 44: 1119–1136.
20. Kumar, R. K., C. Herbert, and P. S. Foster. 2008. The "classical" ovalbumin challenge model of asthma in mice. *Curr. Drug Targets* 9: 485–494.
21. Epstein, M. M. 2004. Do mouse models of allergic asthma mimic clinical disease? *Int. Arch. Allergy Immunol.* 133: 84–100.
22. Molofsky, A. B., J. C. Nussbaum, H.-E. Liang, S. J. Van Dyken, L. E. Cheng, A. Mohapatra, A. Chawla, and R. M. Locksley. 2013. Innate lymphoid type 2 cells sustain visceral adipose tissue eosinophils and alternatively activated macrophages. *J. Exp. Med.* 210: 535–549.
23. Hammad, H., N. Debeuf, H. Aegerter, A. S. Brown, and B. N. Lambrecht. 2022. Emerging paradigms in type 2 immunity. *Annu. Rev. Immunol.* 40: 443–467.
24. Holgate, S. T., S. Wenzel, D. S. Postma, S. T. Weiss, H. Renz, and P. D. Sly. 2015. Asthma. *Nat. Rev. Dis. Primers* 1: 15025.
25. Bousquet, J., J. M. Anto, C. Bachert, I. Baiardini, S. Bosnic-Anticevich, G. Walter Canonica, E. Melén, O. Palomares, G. K. Scadding, A. Togias, and S. Toppila-Salmi. 2020. Allergic rhinitis. *Nat. Rev. Dis. Primers* 6: 95.
26. Fuertes, L. V., M. P. Bustamante, A. B. Fernandez, A. G. Pino, and F. P. De La Losa. 2013. A case of eosinophilic esophagitis, with sensitization to BSA (meat allergy) and rhinoconjunctivitis due to dog epithelium. *Clin. Transl. Allergy* 3(Suppl. 3): P166.
27. Morris, D. L., K. W. Cho, J. L. Delproposto, K. E. Oatmen, L. M. Geletka, G. Martinez-Santibanez, K. Singer, and C. N. Lumeng. 2013. Adipose tissue macrophages function as antigen-presenting cells and regulate adipose tissue $CD4^+$ T cells in mice. *Diabetes* 62: 2762–2772.
28. Chen, K. E., N. M. Lainez, M. G. Nair, and D. Coss. 2021. Visceral adipose tissue imparts peripheral macrophage influx into the hypothalamus. *J. Neuroinflammation* 18: 140.
29. Hata, M., E. M. M. A. Andriessen, M. Hata, R. Diaz-Marin, F. Fournier, S. Crespo-Garcia, G. Blot, R. Juneau, F. Pilon, A. Dejda, et al. 2023. Past history of obesity triggers persistent epigenetic changes in innate immunity and exacerbates neuroinflammation. *Science* 379: 45–62.